CHAPTER 6

EFFECT OF STRESS RATIO AND MEAN STRESS ON HIGH CYCLE FATIGUE BEHAVIOR OF SUPERALLOY IN718 AT 600°C

6.1 INTRODUCTION

This chapter present the effect of mean stress on high cycle fatigue behavior of the superalloy IN718 at 600°C, at stress ratios (R) -1, 0.5, and 0.7. There is decrease in fatigue life, with increase in the tensile mean stress. At high mean stress, the decrease in fatigue life is found to be associated with multiple crack initiation sites at the specimen surface. The fatigue limit is found to be strongly affected by the tensile mean stress and stress ratio, R=0.7, since the maximum stress approaches near the yield stress and causes cyclic ratcheting.

6.2 RESULTS

6.2.1 EFFECT OF MEAN STRESS ON HIGH CYCLE FATIGUE

The effect of mean stress on the allowable stress amplitude for affixed number of cycles was evaluated using the following equations [Dieter and Bacon, (1986)]:

Goodman equation: $\quad \sigma_a = \sigma_e \left[1 - (\sigma_m / \sigma_u)\right]$ (6.1)

Soderberg equation: $\quad \sigma_a = \sigma_e \left[1 - (\sigma_m / \sigma_y)\right]$ (6.2)

Gerber parabola: $\sigma_a = \sigma_e \left[1 - (\sigma_m / \sigma_u)^2 \right]$ (6.3)

where σ_a is stress amplitude, σ_e is endurance strength, σ_m is mean stress, σ_y is yield strength and σ_u is ultimate tensile strength.

Table 6.1: Comparison of actual and calculated values of the stress amplitudes at different mean stresses corresponding to R = 0.5 and 0.7 for 10^6 cycles.

R	σ_{max} (MPa)	σ_{min} (MPa)	σ_m (MPa)	$(\sigma_a)_{actual}$ (MPa)	$(\sigma_a)_{Goodman}$ (MPa)	$(\sigma_a)_{Soderberg}$ (MPa)	$(\sigma_a)_{Gerber}$ (MPa)
0.5	1008	504	756	252	232	185	383
0.7	1000	700	878	155	164	110	362

$\sigma_y = 1058$ MPa, $\sigma_u = 1176$ MPa and $\sigma_e = 650$ MPa for 10^6 cycles.

The experimental values of the stress amplitudes for R = 0.5 and R = 0.7, corresponding to fatigue life of 10^6 cycles, are shown in Table 6.1. It may be seen that the values estimated from Goodman equation are closest to the actual values of the applied stress amplitude.

The variation of fatigue life (N_f) with stress amplitude at 600ºC, under symmetric loading (R= -1) at frequency of 30Hz is shown in Fig. 6.1. There is decrease in fatigue life with increase in the stress. The fatigue strength corresponding to 10^7 cycles is around 550 MPa under symmetric loading (R= -1), on the other hand under asymmetric loading fatigue strength is reduced to 234 and 124 MPa for R = 0.5 and 0.7 respectively. The arrows marked in Fig. 6.1 corresponds to samples which have not failed till 10^7 cycles. The Nicholas–Haigh diagram shown in Fig. 6.2 presents the effect of maximum stress on plastic strain accumulation. In order to investigate the effect of mean stress on ratcheting strain and fatigue life at high stress ratio, fatigue tests are conducted at

different mean stresses by varying maximum and minimum stress. Ratcheting fatigue life of specimen for mean stresses 900, 950 and 1000 MPa are 1.34×10^6, 8.43×10^5 and 2.92×10^4 cycles respectively.
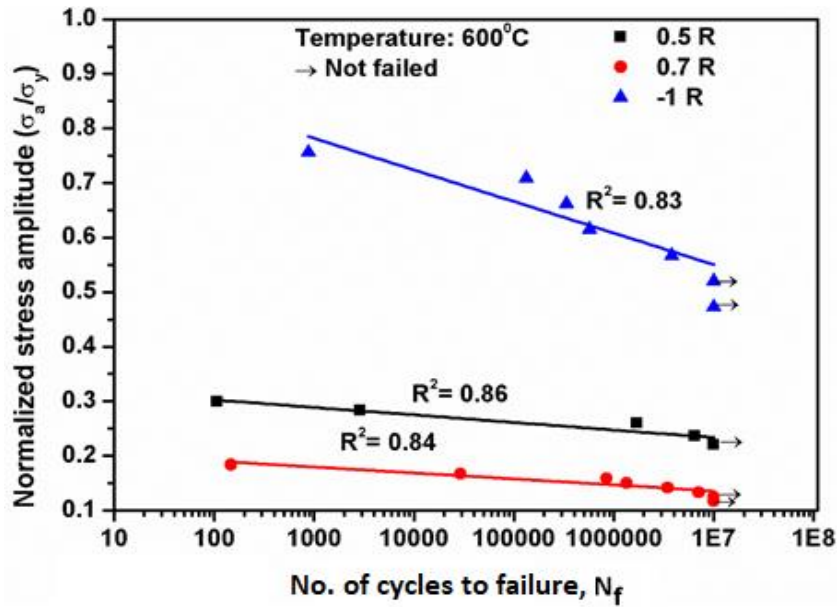
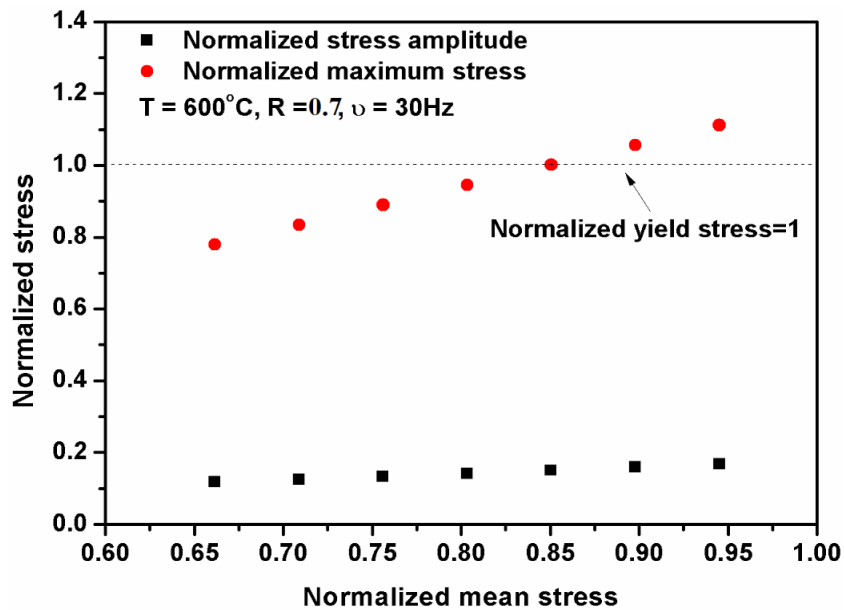**Fig. 6. 1:** Effect of stress ratio on fatigue life at 600°C.

Fig. 6. 2: Nicolas Haigh diagram: Maximum stress and stress amplitude vs mean stress at R=0.7, at 600°C.
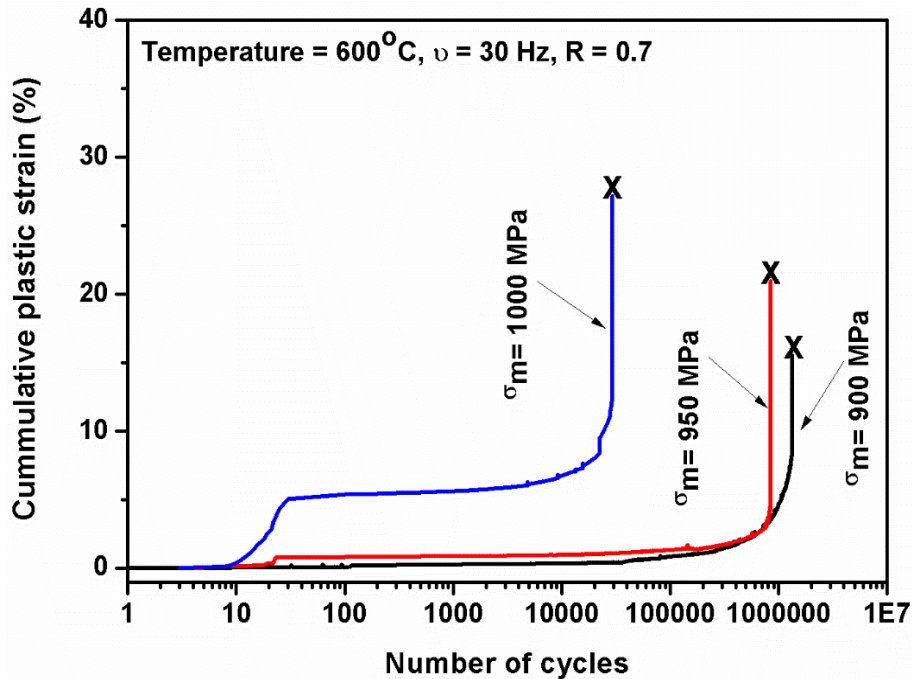
Fig. 6. 3: Effect of mean stress on plastic strain accumulation in the superalloy IN718 with number of cycles at R= 0.7 and 600°C showing variation of cumulative plastic strain with number of cycles.

The variation of cumulative plastic strain with number of cycles for different mean stresses is shown in Fig. 6.3. It is observed that as the mean stress increased the ratcheting strain accumulation also increased. During the initial 10 cycles, the strain is negligible at all the mean stresses, however it starts rising rapidly until 30 cycles., after 30 cycles strain accumulation occurs at a constant rate till $3.5X10^4$, $1.4X10^5$ and $4.8X10^3$ cycles and there is relatively faster increase in plastic strain accumulation till $1.3X10^6$, $8.2X10^5$ and $2.8X10^4$ cycles at the mean stresses of 900, 950 and 1000 MPa respectively. Thereafter, there is drastic increase in the plastic strain accumulation, leading to overload fracture of the specimens. This type of failure is clearly seen in Fig. 6.9 with overload fracture showing dimples. Since, the most detrimental effect on fatigue life is observed for R=0.7, the results pertaining to this stress ratio are discussed in detail.

6.2.2 FRACTURE BEHAVIOR

Figs. 6.4 and 6.5 show SEM fractographs of the samples tested at stress amplitudes of ±600 and ±800 MPa under symmetric cyclic loading (R= -1) at 600ºC. It may clearly be seen that there are multiple crack initiation sites (marked with arrows) in Fig. 6.4 (a) and the interstriation spacing is small (Fig. 6.4 b) in the specimen tested at lower stress amplitude of ±600 MPa. The crack initiation sites on fracture surface of the specimen tested at higher stress amplitude is shown in Fig. 6.5 (a). It may be seen that the interstriation spacing in Fig. 6.5 (b) is larger.
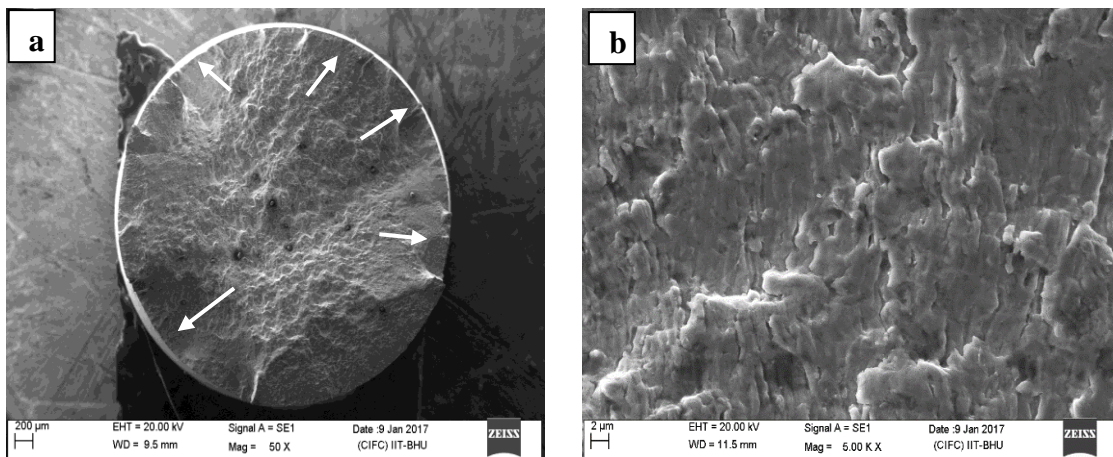

Fig. 6. 4: Fractographs of the sample fractured at the stress amplitude of ±600 MPa (R= -1) at 600ºC showing: (a) the fracture surface and crack initiation site, (b) transgranular crack propagation and fatigue striations with smaller interstriation spacing.
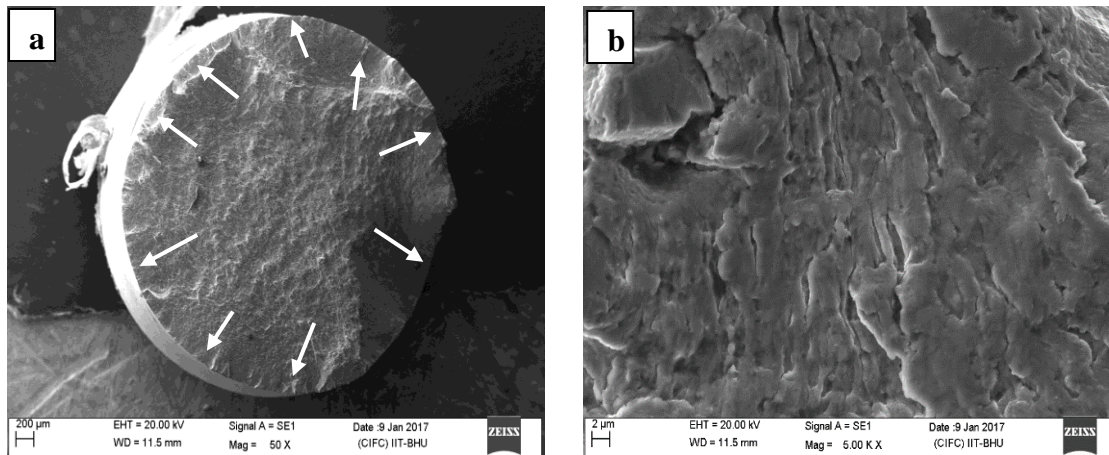
Fig. 6. 5: Fractographs of the sample fractured at the stress amplitude of ±800 MPa (R= -1) at 600ºC showing: (a) the fracture surface and crack initiation site, (b) transgranular crack propagation and fatigue striations with larger interstriation spacing.
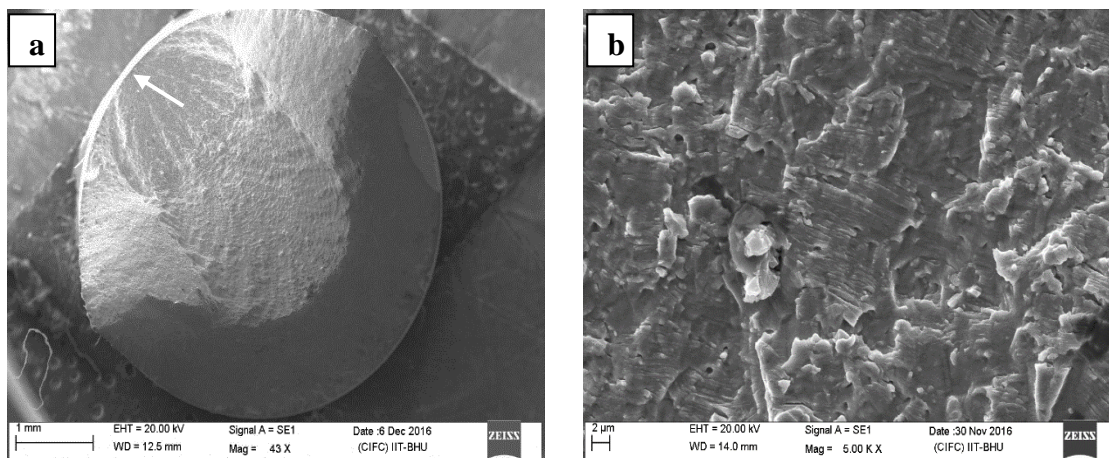

Fig. 6. 6: Fractographs of the sample fractured at the mean stress of 750 MPa (R = 0.5) at 600ºC showing: (a) the fracture surface and crack initiation site, (b) transgranular crack propagation and fatigue striations.

Fig. 6. 7: Fractographs of the sample fractured at the mean stress of 900 MPa (R = 0.5) at 600ºC showing: (a) the fracture surface and crack initiation site, (b) transgranular crack propagation and fatigue striations.
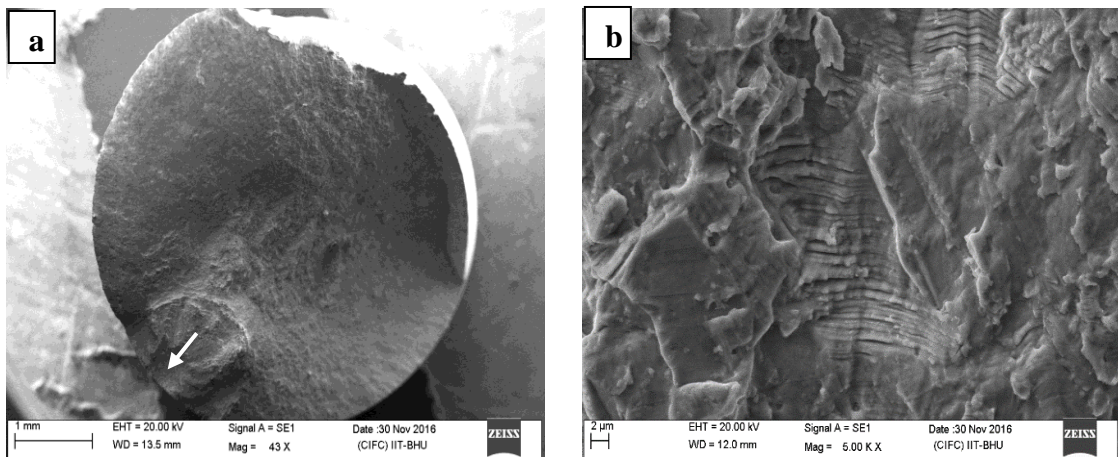

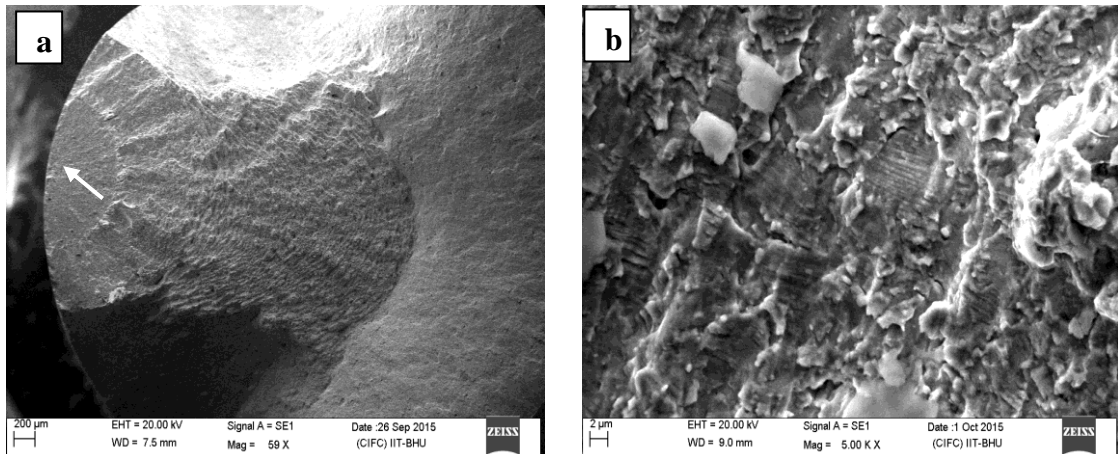
Fig. 6. 8: Fractographs of the sample fractured at the mean stress of 900 MPa (R = 0.7) at 600ºC showing: (a) the fracture surface and crack initiation sites, (b) mixed mode of fracture with fatigue striations and dimples.
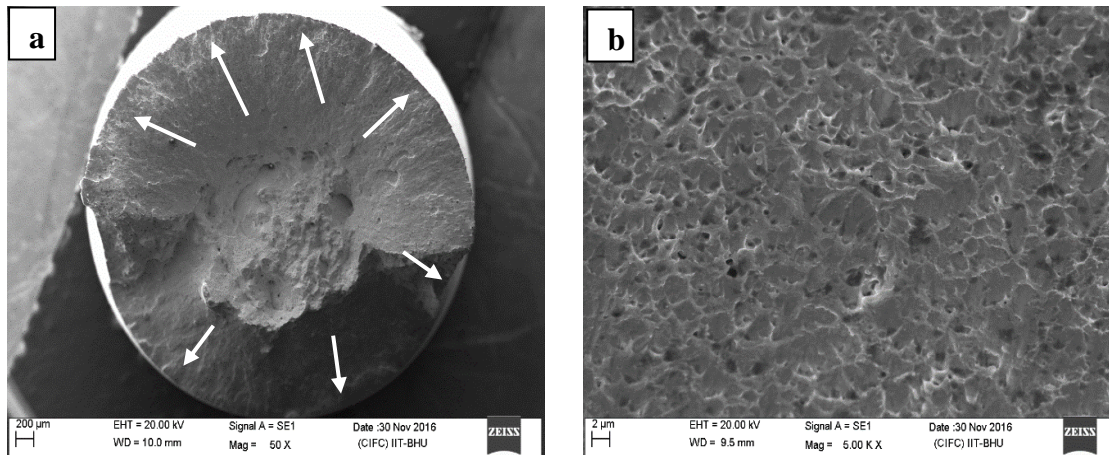
Fig. 6. 9: Fractographs of the sample fractured at the mean stress of 950 MPa (R = 0.7) at 600ºC showing: (a) the fracture surface and crack initiation sites, (b) overload fracture showing dimples.

The SEM fractographs of the samples tested at 600ºC at R = 0.5 and mean stresses of 750 MPa and 900 MPa are displayed in Figs. 6.6 and 6.7, respectively. At the lower mean stresses, there is single crack initiation site (Figs. 6.6 -6.7). SEM fractographs of the samples tested at 600ºC at R = 0.7, at the mean stresses of 900 MPa and 950 MPa are shown in Fig. 6.8 and 6.9, respectively. At the higher mean stress the specimens failed from overload with multiple crack initiation sites (Fig. 6.9).

6.3 DISCUSSION

Fatigue life is strongly affected by the loading variables such as stress amplitude, test temperature and mean stress. Increase in temperature not only reduces the fatigue strength but also accelerates the rate of oxidation. To investigate the effect of stress amplitude and stress ratio on high cycle fatigue life, fatigue tests were conducted at different mean stresses by varying the stress ratio at 600°C. The variation of stress

amplitude with the number of cycles for different mean stresses and stress ratios is shown in Fig. 6.1. It is seen that with increase in the stress amplitude the number of cycles to failure decreases. Furthermore, from Fig. 6.1, it is evident that the stress amplitude (σ_a) increases with decrease in the value of R, which is in agreement with the earlier investigation **[Mikado et al. (2014)]**. Tensile mean stress is known to reduce the stress range for the specific fatigue life whereas compressive mean stress increases the allowable stress range for the specific fatigue life **[Dieter et al. (1986)]**. The decrease in the stress range with increase in the mean stress is the major cause of fatigue failure. The Nicholas–Haigh diagram, presents stress amplitude and maximum stress as a function of mean stress for constant fatigue life (Fig. 6.2). At higher stress ratios, the maximum stress approaches the yield stress and causes cyclic ratcheting. Fig. 6.3 shows the cumulative plastic strain versus number of cycles plot for the specimens tested at the different mean stresses and constant stress ratio (R=0.7). Cyclic ratchetting is the main reason for the elongation of the specimens, when maximum stress is above the yield stress (Fig. 6.2). In general, initially there is rapid increase in the cumulative plastic strain, followed by linear increase at a constant rate, and finally there is failure due to large accumulated plastic strain **[Morrissey et al. (1999)]**. The plastic strain accumulation increases rapidly with increase in the tensile mean stress. **Kang et al. (2011)** reported similar observation, in which increase in the tensile mean stress led to reduction in fatigue life due to increase in the accumulated plastic strain.

Figs. 6.4 - 6.9 show the overall view of the fracture surfaces at different stress levels with fatigue crack initiation sites marked with arrows. Fatigue cracks initiated from surface of the specimens at different stress levels. The inter-striation spacing increases with increase in the stress amplitude for R = -1. Examination of fracture surfaces of the

HCF tested samples at R= -1, revealed crack initiation sites along the periphery of the fractured surfaces. At high stress amplitude, fatigue cracks initiated from multiple initiation sites, the number of crack initiation sites was larger at high stress amplitude and it decreased at lower stress amplitude (Fig. 6.4). At a higher stress level (Fig. 6.5 b) few secondary cracks appear which are normal to the main fatigue crack propagation and situated at grain boundaries. Similar results are also observed by **Belan (2015)**. The regions of fatigue crack growth are evident from the distinct fatigue striations, in the transgranular mode of fatigue crack propagation.

Figs. 6.6 – 6.7 show SEM fractographs of the samples failed at R = 0.5 at 600ºC. Here also transgranular mode of fatigue crack propagation is observed. Figs. 6.8 – 6.9 show SEM fractographs of the samples failed at R = 0.7 at 600ºC. The spacing between the striations increases with increase in the tensile mean stress. Fig. 6.7 (b) shows transgranular mode of fatigue crack propagation, whereas Fig. 6.8 (b) shows a mixed mode of fracture with fatigue crack propagation and dimples. Fig. 6.9 (b) shows dimples without fatigue striation and the specimens failed in overload with multiple crack initiation sites at the higher mean stresses. From Fig. 6.1, it can be seen that the maximum stress is above the yield strength at R=0.7; therefore, there may be a possibility of accumulation of strain due to cyclic ratcheting, leading to fracture with appearance of dimples, which has been reported also earlier **[Morrissey et al. (1999), Rajpurohit et al. (2018)]**.

6.4 CONCLUSIONS

The following conclusions can be drawn from this study on the effect of stress ratio and mean stress on high cycle fatigue of the superalloy IN718 at 600ºC:

a) The fatigue strength corresponding to 10^7 cycles is around 550 MPa under symmetric loading (R= -1), on the other hand under asymmetric loading fatigue strength is reduced to 234 and 124 MPa for R = 0.5 and 0.7 respectively.

b) At R = -1, the decrease in fatigue life is attributed to multiple crack initiation sites at the surface. The fatigue crack propagation from the surface of the specimen is revealed by striations.

c) At higher mean stresses the decrease in fatigue life is attributed to multiple crack initiation sites at the surface for R = 0.7 due to strain accumulation.